International Journal of Mechanical Engineering (IJME)
ISSN 2319-2240
Vol. 2, Issue 2, May 2013, 69-86

International Academy of Science, Engineering and Technology
Connecting Researchers; Nurturing Innovations

NUMERICAL SOLUTION OF FLUID FLOW THROUGH A ROTATING RECTANGULAR STRAIGHT DUCT WITH MAGNETIC FIELD

KAMRUZZAMAN[1], MOHAMMAD WAHIDUZZAMAN[2], MAHMUD ALAM[3], M. FERDOWS[4], MOTALEB HOSSAIN[5] & RAUSHAN ARA QUADIR[6]

[1,2,3]Mathematics Discipline, Khulna University, Khulna, Bangladesh

[4,5]Department of Mathematics, University of Dhaka, Dhaka, Bangladesh

[6]School of Mathematics, Statistics and Computer Science, University of KwaZulu-Natal, Durban, South Africa

ABSTRACT

In this paper fluid flow through a rotating rectangular straight duct in the presence of magnetic field under various flow conditions is investigated by using numerical techniques. Although the Spectral method is applied as a main numerical tool, the Chebyshev polynomial, the Collocation method and the Newton-Raphson method are also used as secondary tools. The Magnetohydrodynamics incompressible viscous steady fluid flow through a straight duct of rectangular cross-section rotating at a constant angular velocity about the center of the duct cross-section is investigated numerically to examine the combined effects of Magnetic parameter (M_g), Taylor number (T_r), Pressure Gradient Parameter (D_n) and aspect ratio $(\gamma)=\frac{b}{a}$ where a is the half width of the duct cross-section, b is the half height of the duct, Ω is the angular velocity, μ is the viscosity, υ is the kinematic viscosity. One of the interesting phenomena of the flow is the solution curve and the flow structure. The flow structures in case of rotation of the duct axis and the Pressure Gradient with large Magnetic force number as well as large Taylor number have been examined while other parameters remain constant. The calculation are carried out for $5 \le M_g \le 50000, 50 \le T_r \le 100000, D_n =$ 500, 1000, 1500 and 2000 where the aspect ratio $\gamma = 2.0$. For high magnetic parameter and large Taylor number, almost all the fluid particles strength is weak. The maximum axial flow will be shifted to the center from the wall and turn into the ring shape.

KEYWORDS: Rotating Rectangular Straight Duct, Magnetohydrodynamics, Duct Cross-Section

INTRODUCTION

Fluid flow in a straight duct is of great importance. It has large applications both in chemical and mechanical engineering. A lot of research works regarding fully developed flow have been carried out at different times. The aim of this paper is to make some numerical calculations on the fluid flow in a rotating rectangular straight duct in the presence of magnetic field which has many engineering and industrial applications. The results of these investigations may not have direct practical applications but are relevant to the problems mentioned above. The fluid flow through a rectangular straight duct rotating at a constant angular velocity about an axis normal to a plane including the duct is subjected to both Coriolis and centrifugal forces. Such rotating passages are used in cooling systems for conductors of electric generators. Flow in a rotating straight pipe is of interest because the secondary flows in this case are qualitatively similar to those in stationary curved system in view of the similar centrifugal mechanism including the secondary curved systems (Ishigaki (1955)). The earliest work on the flow in rotating straight pipe was carried out for the asymptotic limits of weak and strong rotations by Barua (1955). Benton & Baltimore (1956) used a perturbation expansion to the Hagen-Poiseuille flow. The study of Mori

and Nakayama (1983), Ito and Nanbu (1971), Wanger and Velkoff (1994) for small rotational speed and high axial pressure gradient resulted good agreement with experiments, showing an increases in friction factor with rotational speed. Alam, Begum and Yamamoto (2007) have used spectral method to describe the flow through a rotating straight pipe with large aspect ratio. MHD flow in an insulating rectangular duct under a non-uniform magnetic field is studied by Moreau *et al.* (2010). Numerical solutions of MHD flows past obstacles in a duct under externally applied magnetic field is studied by Dousset.V (2009). Zengyu*et al.*(2005) investigates the study of surface and bulk instabilities in MHD duct flow with imitation of insulator coating imperfection. Hence our aim is to study the numerical solution of fluid flow through a rotating rectangular straight duct in the presence of magnetic field. The Spectral method is used as the main tool and the Chebyshev polynomial, the Newton-Raphson method and the Collocation method are used as secondary tools to obtain the numerical solution.

GOVERNING EQUATION

The fully developed laminar flow of an incompressible viscous fluid in a straight duct that is subjected to a steady rotating $\mathbf{\Omega}$ with rectangular cross-section in the presence of magnetic field has been considered. Let $2a$ is the width of the duct cross-section and $2b$ its height. Cartesian co-ordinate system (x', y', z') has been considered to describe the motion of the fluid particles in the duct and same co-ordinate also (x', y', z') with the center O in a rectangular cross-section of the duct which is illustrated in Figure 2.1. The system rotates at a constant angular velocity $\mathbf{\Omega} = (0, -\Omega, 0)$ around the $y' -$axis. The flow is drive pressure gradient $-\frac{\partial p'}{\partial z'} = G$ along the centerline of the duct in the presence of magnetic field.

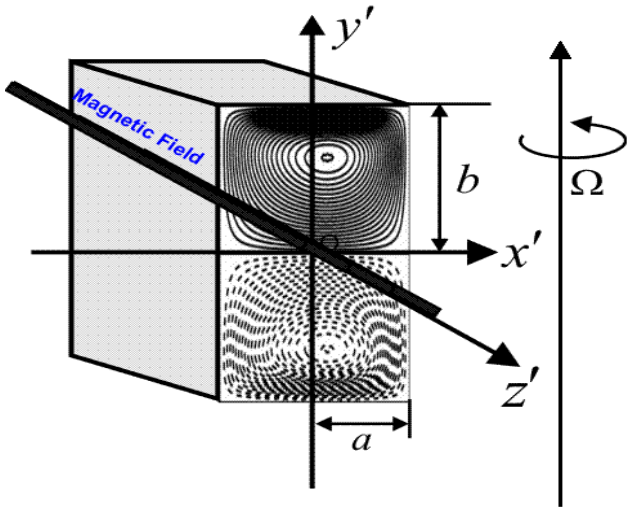

Figure 1: Co-Ordinate System in a Rotating Straight Duct

u', v', w' are the dimensional velocity components along x', y', z' direction respectively and u, v, w is the dimensionless velocity along x, y, z direction respectively. p' is the modified pressure which includes gravitational and centrifugal force potentials. The velocity $\mathbf{q}$ is a solution of the Navier-Stokes equation and continuity equation which takes the form:

$$\nabla \cdot \mathbf{q} = 0 \tag{1}$$

Then the fluid moves along the electric and magnetic field in a rotating straight duct with rectangular cross-section along the center line is of the form:

$$\frac{\partial \overline{\mathbf{q}}}{\partial t}+\overline{q}\left(\overline{q}\cdot\overline{\nabla}\right)=-\frac{1}{\rho}\left(\overline{\nabla}\cdot\overline{\mathbf{p}}\right)+\upsilon\nabla^{2}\mathbf{q}+2\left(\mathbf{\Omega}\wedge\mathbf{q}\right)+\frac{1}{\rho}\left(\mathbf{J}\wedge\mathbf{B}\right) \tag{2}$$

Where ***J*** is the electric current density, ***B*** is the magnetic induction, Ω is the angular velocity and υ is the kinematic viscosity.

The generalized Ohm's law in the absence of electric field is of the form

$$\mathbf{J}+\frac{\omega_{\mathbf{e}}\tau_{e}}{\mathbf{H}_{0}}\mathbf{J}\wedge\mathbf{B}=\boldsymbol{\sigma}'(\boldsymbol{\mu}_{\mathbf{e}}\mathbf{q}'\wedge\mathbf{H}+\frac{\mathbf{1}}{\mathbf{en}_{\mathbf{e}}}\nabla\mathbf{p}_{e}) \tag{3}$$

where, ω_e is the cyclotron frequency, τ_e is the electron collision, $\mathbf{e}$ is the electric charge, n_e is the number density electron.

Neglecting the Hall current, we have from the equation (3)

$$\mathbf{J}=\sigma'\left(\mu_{e}\mathbf{q}'\wedge\mathbf{H}\right)\left[\because\omega_{e}\tau_{e}=0\text{and}\,p_{e}=0\right] \tag{4}$$

The boundary conditions are that $u'=v'=w'=0$ on the wall of the straight duct. The assumption of fully developed flow means that except for the pressure derivative all z' derivatives are set to zero. For steady flow i.e. $\frac{\partial u'}{\partial t}=\frac{\partial v'}{\partial t}=\frac{\partial w'}{\partial t}=0$ and there is no body force inside the straight duct. Here the axis of rotation is perpendicular to the span of the pipe and the axial pressure gradient $-\frac{\partial p'}{\partial z'}=G$ is constant and is maintained by external means i.e. p' is the modified pressure, which includes the gravitational and centrifugal force potentials. The axial pressure gradient $G=-\frac{\partial p'}{\partial z'}$.

Thus from the equation (1), (2), (3) and (4)

$$u'\frac{\partial u'}{\partial x'}+v'\frac{\partial u'}{\partial y'}=-\frac{1}{\rho}\frac{\partial p'}{\partial x'}+\upsilon\left(\frac{\partial^{2}u'}{\partial x'^{2}}+\frac{\partial^{2}u'}{\partial y'^{2}}\right)-2\Omega w'-\frac{\sigma'B_{0}^{2}}{\rho}u' \tag{5}$$

$$u'\frac{\partial v'}{\partial x'}+v'\frac{\partial v'}{\partial y'}=-\frac{1}{\rho}\frac{\partial p'}{\partial y'}+\upsilon\left(\frac{\partial^{2}v'}{\partial x'^{2}}+\frac{\partial^{2}v'}{\partial y'^{2}}\right)-\frac{\sigma'B_{0}^{2}}{\rho}v' \tag{6}$$

$$u'\frac{\partial w'}{\partial x'}+v'\frac{\partial w'}{\partial y'}=-\frac{1}{\rho}\frac{\partial p'}{\partial z'}+\upsilon\left(\frac{\partial^{2}w'}{\partial x'^{2}}+\frac{\partial^{2}w'}{\partial y'^{2}}\right)+2\Omega u' \tag{7}$$

and

$$\frac{\partial u'}{\partial x'}+\frac{\partial v'}{\partial y'}=0 \tag{8}$$

Now, the dependent and independent variables are then normalized as follows:

$$u' = \frac{\upsilon}{a}u; \quad x' = xa; \quad p' = \frac{\upsilon^2}{a^2}\rho p \; ; \quad v' = \frac{\upsilon}{a}v; \quad y' = ya; \quad w' = \frac{\upsilon}{a}w; \qquad z' = 0$$

where the variables are with prime are dimensional quantities and $"a"$ be the half width of the cross section of the pipe. The boundary condition is that the velocities are zero at $x = \pm 1$ and $y = \pm\left(\frac{b}{a}\right) = \pm\gamma$ (aspect ratio).

We have introduced the new variable $\bar{y} = \left(\frac{y}{\gamma}\right)$, where γ is the aspect ratio i.e. $\gamma = \left(\frac{b}{a}\right)$, where b be the half height of the cross- section and $u = -\left(\frac{\partial \psi}{\partial y}\right)$ and $v = \left(\frac{\partial \psi}{\partial x}\right)$ which satisfies the continuity equation.

We have the basic equation for ψ and w as:

$$\frac{\partial^4\psi}{\partial x^4} + \frac{2}{\gamma^2}\frac{\partial^4\psi}{\partial \bar{y}^2 \partial x^2} + \frac{1}{\gamma^4}\frac{\partial^4\psi}{\partial \bar{y}^4} = -\frac{1}{\gamma^3}\frac{\partial\psi}{\partial\bar{y}}\frac{\partial^3\psi}{\partial\bar{y}^2\partial x} - \frac{1}{\gamma}\frac{\partial\psi}{\partial\bar{y}}\frac{\partial^3\psi}{\partial x^3} + \frac{1}{\gamma^3}\frac{\partial\psi}{\partial x}\frac{\partial^3\psi}{\partial\bar{y}^3} + \frac{1}{\gamma}\frac{\partial\psi}{\partial x}\frac{\partial^3\psi}{\partial x^2\partial\bar{y}}$$

$$-\frac{1}{\gamma}\frac{\partial w}{\partial\bar{y}}T_r + \left(\frac{1}{\gamma^2}\frac{\partial^2\psi}{\partial\bar{y}^2} + \frac{\partial^2\psi}{\partial x^2}\right)M_g \tag{9}$$

$$\frac{\partial^2 w}{\partial x^2} + \frac{1}{\gamma^2}\frac{\partial^2 w}{\partial\bar{y}^2} = -\frac{1}{\gamma}\frac{\partial\psi}{\partial\bar{y}}\frac{\partial w}{\partial x} + \frac{1}{\gamma}\frac{\partial\psi}{\partial x}\frac{\partial\psi}{\partial\bar{y}} - D_n + \frac{1}{\gamma}\frac{\partial\psi}{\partial\bar{y}}T_r \tag{10}$$

where, Rotating parameter $T_r = 2\left(\frac{a^2\Omega}{\upsilon}\right)$, Magnetic parameter $M_g = \frac{\sigma'}{\mu_e}a^2B_0^2 = \sigma'\mu_e a^2 H_0^2$ pressure driven parameter $D_n = \frac{Ga^3}{\rho\upsilon^2}$.

The boundary conditions for ψ and w are given by

$$w(\pm 1, \bar{y}) = w(x, \pm 1) = \psi(\pm 1, \bar{y}) = 0$$

$$\left(\frac{\partial\psi}{\partial x}\right)(\pm 1, \bar{y}) = \psi(x, \pm 1) = \left(\frac{\partial\psi}{\partial\bar{y}}\right)(x, \pm 1) = 0$$

Flux through the Straight Duct

The dimensional total flux Q' through the duct is $Q' = \int_{-b}^{b}\int_{-a}^{a} w\,dx'\,dy' = \upsilon a Q$

where $Q = \int_{-\gamma}^{\gamma}\int_{-1}^{1} w\,dx\,d\bar{y}$ is the non- dimension flux.

Calculation Technique

The present work is based on numerical methods. For this reason the Spectral method is used as a numerical technique to obtain the solution. It is necessary to discuss the method in detail. The basic ideas of the Spectral and the Collocation methods are given below. The expansion by polynomial functions is utilized to obtain steady or un-steady solution. The series of the Chebyshev polynomial is used in the x and $\bar{y}$ directions where, x and $\bar{y}$ are variables. Assuming the flow is symmetric along the axial direction. The expansion function $\phi_n(x)$ and $\psi_n(x)$ are expressed as

$$\phi_n(x) = (1-x^2)T_n(x) \tag{11}$$

$$\psi_n(x) = (1-x^2)^2 T_n(x) \tag{12}$$

where, $T_n(x) = \cos(n\cos^{-1}(x))$ is *n*-th order first kind Chebyshev polynomial.

$w(x,\bar{y})$ and $\psi(x,\bar{y})$ are expanded in terms of the function $\phi_n(x)$ and $\psi_n(x)$ as:

$$w(x,\bar{y}) = \sum_{m=0}^{M}\sum_{n=0}^{N} w_{mn}\phi_m(x)\phi_n(\bar{y}) \tag{13}$$

$$\psi(x,\bar{y}) = \sum_{m=0}^{M}\sum_{n=0}^{N} \psi_{mn}\psi_m(x)\psi_n(\bar{y}) \tag{14}$$

where, M and N are the truncation numbers in the x and $\bar{y}$ directions respectively. The Collocation method (Gottlieb and Orszag, 1977) applied in x and $\bar{y}$ directions yield a set of nonlinear differential equations for w_{mn} and ψ_{mn}. The collocation points are taken as

$$(x_i, \bar{y}_j) \qquad x_i = \cos\left[\pi\left(1-\frac{i}{M+2}\right)\right] \qquad (i = 1,2.....M+1) \tag{15}$$

$$\bar{y}_j = \cos\left[\pi\left(1-\frac{j}{N+2}\right)\right] \qquad (j = 1,2,.....N+1) \tag{16}$$

and the non-linear differential equations are expanded symbolically as

$$A_1 w + B_1 w + c_1 w = N_1(w_{mn}, \psi_{mn}) \tag{17}$$

$$A_2 \psi + B_2 \psi + c_2 \psi = N_2(w_{mn}, \psi_{mn}) \tag{18}$$

where, A_1, B_1, C_1 and A_2, B_2, C_2 are squares matrices with $(M+1)(N+1)$ dimension. $w = (W_{00}, W_{M0}.....W_{0N}.....W_{MN})$ and $\psi(\psi_{00}.....\psi_{M0}.....\psi_{0N}.....\psi_{MN})$, N_1, N_2 are the non-linear operators. The obtained non-linear algebraic equations are solved by the Newton-Raphson iteration method as follows:

$$w^{(p+1)} = C_1^{-1} N_1(w_{mn}^{(p)}, \psi_{mn}^{(p)}) \tag{19}$$

$$\psi^{(p+1)} = C_2^{-1} N_2(w_{mn}^{(p)}, \psi_{mn}^{(p)}) \tag{20}$$

where p denotes the iteration number. In order to avoid difficulty near the point of inflection for the steady solution, the arc-length method is used. In the arc- length method, the arc-length 'S' plays a central role in the formulation. The arc-length equation is

$$\sum_{m=0}^{M}\sum_{n=0}^{N}\left[\left(\frac{dw_{mn}}{ds}\right)^2 + \left(\frac{d\psi_{mn}}{ds}\right)^2\right] = 1 \tag{21}$$

which is solved simultaneously with equations (19) and (20) by using the Newton-Raphson iteration method. An initial guess at a point $s + \Delta s$ is considered starting from point s as follows

$$w_{mn}(s + \Delta s) = w_{mn}(s) + \frac{dw_{mn}(s)}{ds}\Delta s \tag{22}$$

$$\psi_{mn}(s + \Delta s) = \psi_{mn}(s) + \frac{d\psi_{mn}(s)}{ds}\Delta s \tag{23}$$

To obtain a correct solution at $s + \Delta s$, an iteration is carried out. The convergence is assumed by taking sufficiently small $\in_p$ $(\in_p < 10^{-8})$ defined as:

$$\in_p = \sum_{m=0}^{M}\sum_{n=0}^{N}\left[(w_{mn}^{(p+1)} - w_{mn}^{(p)})^2 + (\psi_{mn}^{(p+1)} - \psi_{mn}^{(p)})^2\right] \tag{24}$$

The basic equations and the boundary conditions allow us to get a symmetric solution with respect to the horizontal line passing through the axial direction.

RESULTS AND DISCUSSIONS

Fully developed flow through a rotating rectangular straight duct in the presence of magnetic field is considered for the present investigation. The main flow is forced along the central line and the axis is perpendicular to the span of the duct which has been shown in figure 1. By the definition of Taylor number, the positive rotation means that the direction is the same as the flow and it's called the co-rotation and the negative rotation indicates that the rotation direction is opposite to the main flow direction and is called the counter-rotation.

Steady laminar flow for viscous incompressible fluid has been analyzed under the action of the large magnetic force number (M_g), Dean number (D_n) and Taylor number (T_r) as well as fixed aspect ratio (γ). The main aim of this paper to find out the flow phenomena varying large magnetic force number (M_g) and Dean number (D_n) while the aspect ratio (γ) is remain fixed. For the above mentioned purposes we consider the three cases , *Case* I : $M_g = 5000$ and $D_n = 500, 1000, 1500 \text{and} 2000$; *Case* II : $M_g = 4000$ and $D_n = 500, 1000, 1500 \text{and} 2000$; *Case* III : $M_g = 3000$ and $D_n = 500, 1000, 1500 \text{and} 2000$. Thus interesting and complicated flow behavior of the above mention three cases will be expected. First, the accuracy of the numerical calculation is investigated for the truncation numbers M and N are used in this investigation. For a good accuracy of the solutions, N is chosen equal to γM,

where, γ is the aspect ratio of the duct cross section. After a detail investigation over the truncation numbers, it is concluded that the values M= 10 and N= 20 give sufficient accuracy for the present numerical calculations, the details are not given here for brevity. The steady solution curves have been obtained by the graphical representation of the total flux (Q) versus Taylor number (T_r) at Magnetic parameter $(M_g) = 5000,\ 4000,\ 3000$ corresponding Dean number $(D_n) = 500,\ 1000,\ 1500$ and 2000 respectively where aspect ratio $\gamma = 2.0$.

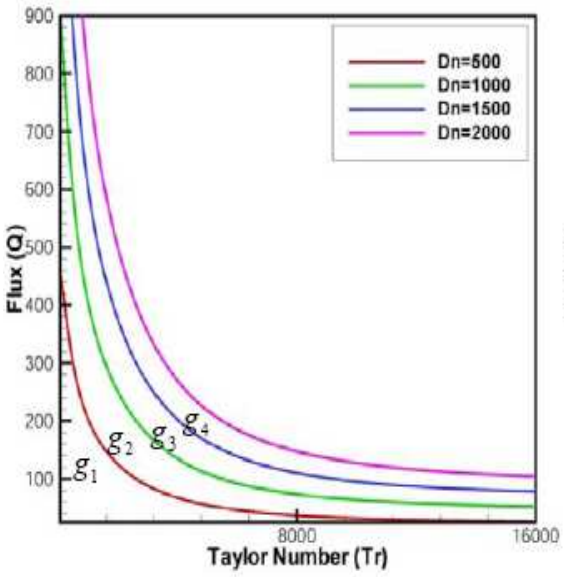

Figure 2: Steady Solution Curve for $\gamma = 2.0,\ M_g =$ 5000, $D_n =$ 500, 1000, 1500 and 2000 and $50 \le T_r \le 16000$

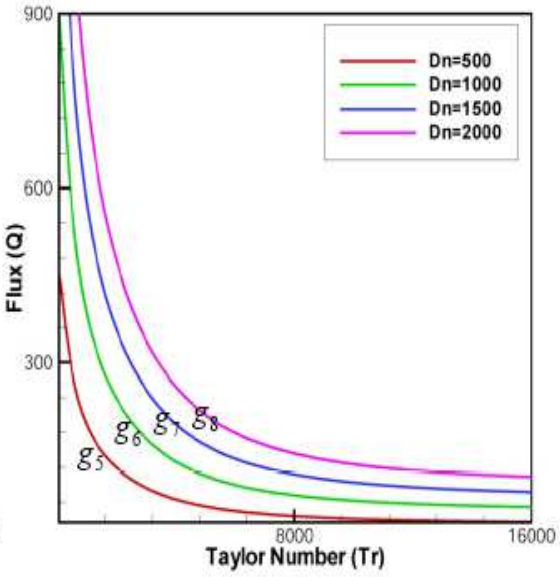

Figure 3: Steady Solution Curve for $\gamma = 2.0,\ M_g =$ 4000, $D_n =$ 500, 1000, 1500 and 2000 and $50 \le T_r \le 16000$

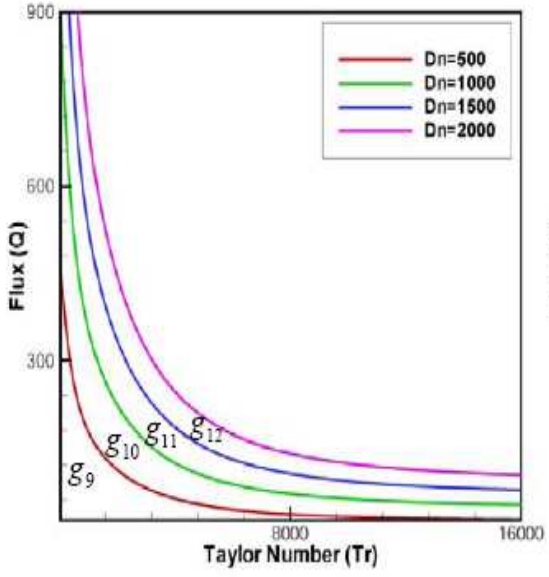

Figure 4: Steady Solution Curve for $\gamma = 2.0,\ M_g =$ 3000, $D_n =$ 500, 1000, 1500 and 2000 and $50 \le T_r \le 16000$

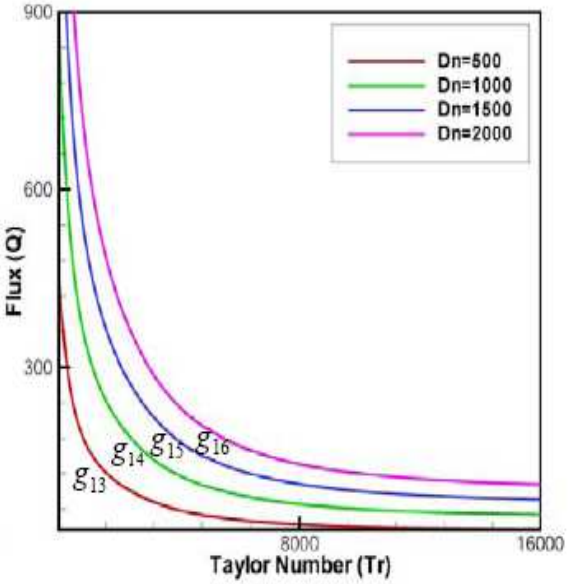

Figure 5: Steady Solution Curve for $\gamma = 2.0,\ M_g =$ 2000, $D_n =$ 500, 1000, 1500 and 2000 and $50 \le T_r \le 16000$

The steady solution curves have been drawn by the path continuation technique in the range $50 \le T_r \le 100000$. The graphical representation has been shown in Figures (4.33(a)-(4.33(e)), for the total flux (Q) versus Taylor number (T_r) in the range $50 \le T_r \le 16000$. For sufficient accuracy, we have considered $M = 10$ and $M = 20$ in the numerical calculations.

Case I: $M_g = 5000$

The steady solution curves have been obtained for aspect ratio $(\gamma) = 2.0$ and $M_g = 5000$ in the range $50 \le T_r \le 32000$ which has been shown in the Figures (6)-(9). These solution curves denoted by g_1, g_2, g_3 and g_4 at the Dean number $(D_n) = 500$, 1000, 1500 and 2000 respectively for graph of the total flux (Q) versus Taylor number (T_r). The flow pattern of the secondary flow and contours plot of the axial flow at several Taylor number (T_r) on the solution curve for constant ψ and w which has been shown in the Figures (6)-(9). we look at the figures from the upstream. Therefore in these figures, we can understand the structures of the secondary flow and the axial flow. We take $T_r =$ (1000, 1500, 1700, 2000, 2300, 2500, 2700, 3500, 3700, 5000, 5500,8000, 1600, 24000) on g_1 curve (see Figure 6); $T_r =$ (1000, 1500, 2000, 2500, 3000, 3700, 4000, 4700, 5000, 7000, 8000, 16000, 24000 and 32000) on g_2 curve (see Figure 7); $T_r =$ (1000, 1500, 2000, 2500, 3000, 3500, 3700, 4700, 5000, 7000, 8000, 16000, 24000 and 32000) on g_3 curve (see Figure 8); $T_r =$ (1000, 1700, 2300, 3000, 3500, 3700, 4300, 5500, 7700, 8700, 16000, 24000 and 32000) on g_4 curve (see Figure 9) where the stream lines of the secondary flow (top) and the contour plots of the axial flow (bottom) in each row from left to the right with the increment $\Delta\psi =$ 0.020, 0.055, 0.075, 0.10 and $\Delta w =$ 8.0, 10.0, 15.0, 16.0 at Dean number $(D_n) = 500$, 1000, 1500 and 2000 respectively. In Figures (6)-(9), the secondary flow, solid lines $(\psi \ge 0)$ show that the secondary flow is the counter clock wise direction and the dotted ones $(\psi < 0)$ show that the secondary flow is in the clock wise direction. We observed that the symmetric solution is obtained in the range $50 \le T_r \le 32000$. The stream lines of the secondary flow are shown at various Taylor number (T_r) in the development of the vortex.3-votex solution has been found at $T_r = 8000$ and 4-vortex solution has been found at $T_r =$ 1000 (with minor one vortex), 1500, 1700, 2300, 2500, 2700, 3500, 3700, 5000, 5500, 6000 (see Figure 6); 2-vortex solutions has been found at $T_r = 16000$ and 3-vortex solution has been found at $T_r =$ 7000, 6000 as well as 4-vortex solutions have been obtained at $T_r =$ 1000 (with one minor vortex), 1500, 2000, 2500, 3000, 3700, 4000, 4700, 5000 (see Figure 7); 2-vortex solution has been found at $T_r = 16000$ and 3-vortex solutions have been found at $T_r =$ 7000, 8000 as well as 4-vortex solutions have been found at $T_r =$ 1000 (with one minor vortex), 1500, 2000, 2500, 3000, 3500, 3700, 4700, 5000 (see Figure 8); 2-vortex solution has been found at $T_r = 16000$ and 3-vortex solution have been found at $T_r =$ 7700, 8700 as well as 4-vortex solution have been found at $T_r =$ 1000 (with one minor vortex), 1700, 2300, 2700, 3000, 3500, 3700, 4300, 5500 (see Figure 9) in the secondary flow patterns. The contour plots of the axial flow has been formed the rings which are either single or double ring shape that appeared depends on the various Taylor number (T_r) as

well as Magnetic parameter (M_g). Single nine rings are found at $T_r = 16000$ and 32000 where Dean number $(D_n) = 500$ in Figure 6; triple nine rings are found at $T_r = 8000$ and double rings are found at $T_r = 16000$, 32000 at Dean number $(D_n) = 1000$, 1500, 2000 respectively.

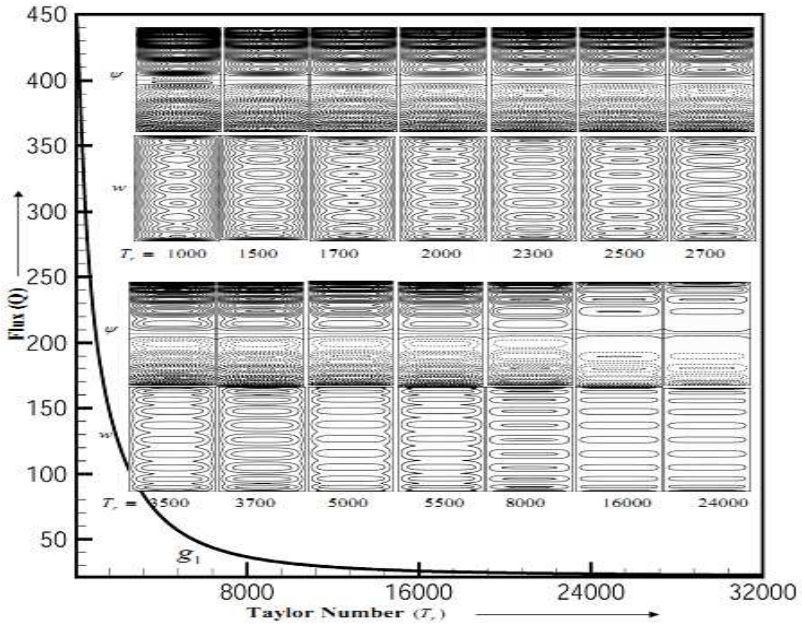

Figure 6: Stream Lines of the Secondary Flow (Top) and Contours Plot of Axial Flow (Bottom) in Each Row at Dean Number $(D_n) = 500$ and $M_g = 5000$ For Flux (Q) versus Taylor Number (T_r) at $T_r = 1000$, 1500, 1700, 2000, 2300, 2500, 2700, 3500, 3700, 5000, 5500, 8000, 16000, 24000

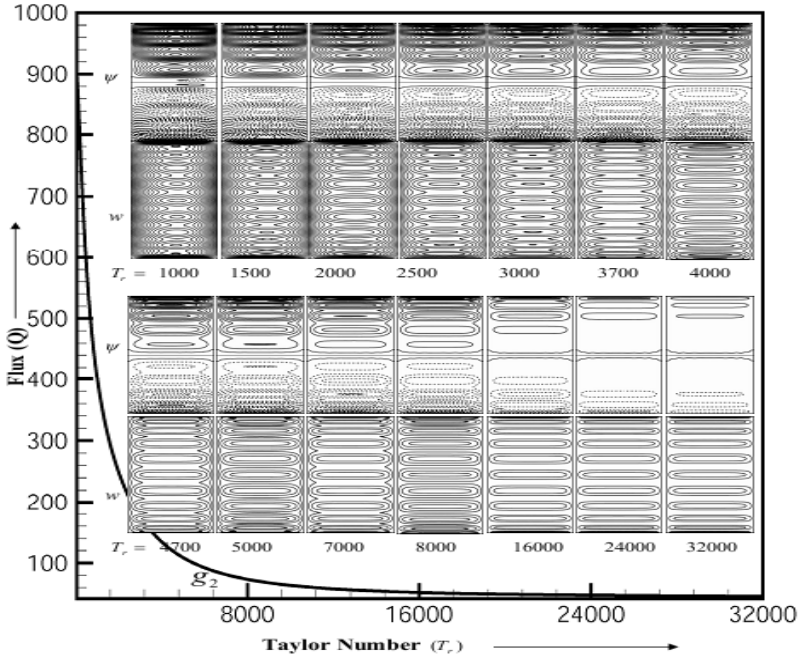

Figure 7: Stream Lines of the Secondary Flow (Top) and Contours Plot of Axial Flow (Bottom) in Each Row at Dean Number $(D_n) = 1000$ and $M_g = 5000$ for Flux (Q) versus Taylor Number (T_r) at $T_r = 1000$, 1500, 2000, 2500, 3000, 3700, 4000, 4700, 5000, 7000, 8000, 16000, 24000, 32000

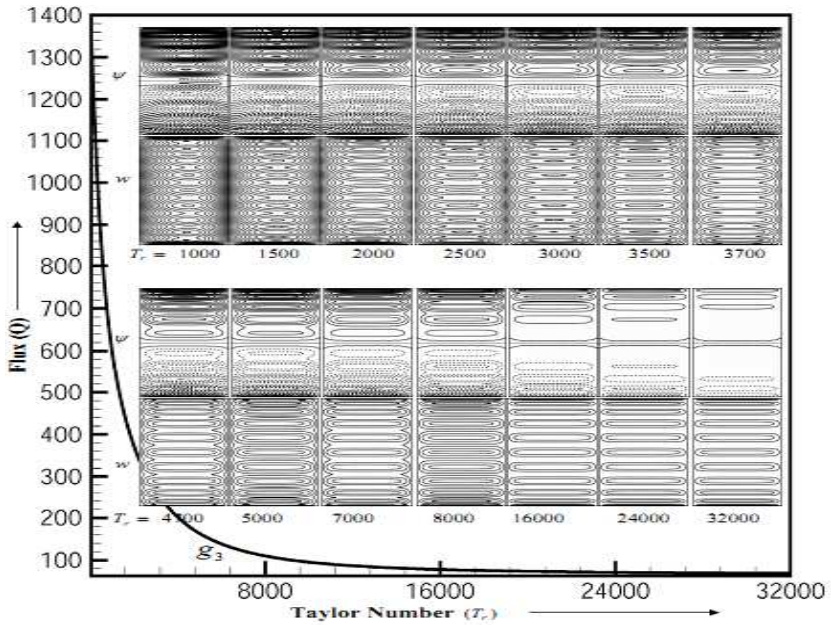

Figure 8: Stream Lines of the Secondary Flow (Top) and Contours Plot of Axial Flow (Bottom) in Each Row at Dean Number $(D_n) = 1500$ and $M_g = 5000$ for Flux (Q) versus Taylor Number (T_r) at $T_r = 1000, 1500, 2000, 2500, 3000, 3500, 3700, 4700, 5000, 7000, 8000, 16000, 24000, 32000$

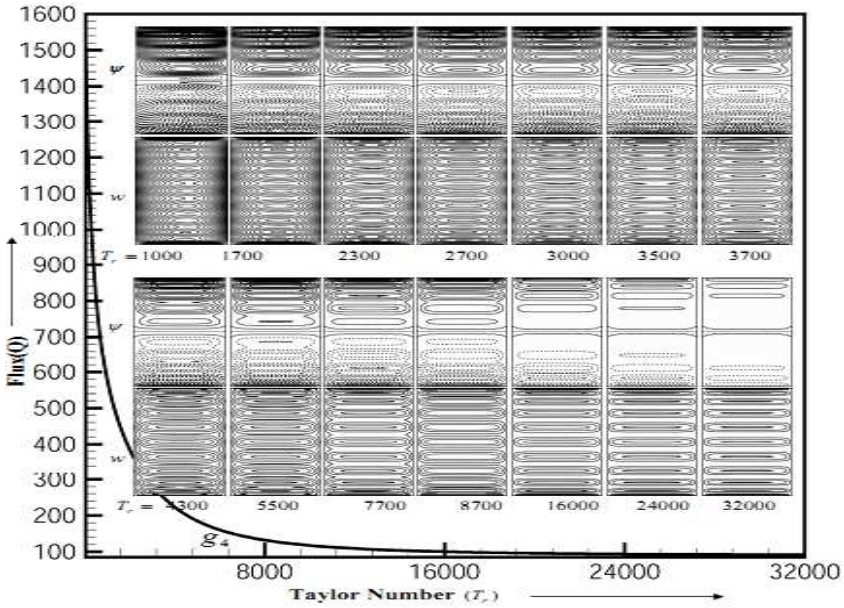

Figure 9: Stream Lines of the Secondary Flow (Top) and Contours Plot of Axial Flow (Bottom) in Each Row at Dean Number $(D_n) = 2000$ and $M_g = 5000$ for Flux (Q) versus Taylor Number (T_r) at $T_r = 1000, 1700, 2300, 2700, 3000, 3500, 3700, 4300, 5500, 7700, 8700, 16000, 24000, 32000$

Case II: $M_g = 4000$

The steady solution curves have been obtained for aspect ratio $(\gamma) = 2.0$ and $M_g = 4000$ in the range $50 \le T_r \le 32000$ which has been shown in the Figures (10)-(13). These solution curves denoted by g_5, g_6, g_7 and

g_8 at the Dean number $(D_n) = 500$, 1000, 1500 and 2000 respectively for graph of the total flux (Q) versus Taylor number (T_r). The flow pattern of the secondary flow and contours plot of the axial flow at several Taylor number (T_r) on the solution curve for constant ψ and w which has been shown by Figures (10)-(13). We look at the figures from the upstream.

Therefore in these figures, we can understand the structures of the secondary flow and the axial flow. We take $T_r = (1000,1300, 2000, 2300, 3000, 3500, 3700, 5500, 8000, 10000, 16000, 20000, 24000$ and $32000)$ on g_5 curve (see Figure 10); $T_r = (1000, 1300, 2500, 3000, 3300, 3700, 4000, 4700, 5000, 7000, 8000, 16000, 24000$ and $32000)$ on g_6 curve (see Figure 11); $T_r = (1000, 1500, 2000, 2500, 3000, 3500, 3700, 4700, 5000, 7000, 8000, 16000, 24000$ and $32000)$ on g_7 curve (see Figure 12); $T_r = (1000, 1300,2000, 2700, 3000, 3700, 4700, 5300, 5500, 5700, 8000, 16000,$ 24000 and $32000)$ on g_8 curve (see Figure 13) where the stream lines of the secondary flow (top) and the contour plots of the axial flow (bottom) in each row from left to right with the increment $\Delta\psi = 0.020, 0.055, 0.075, 0.10$ and $\Delta w = 8.0,$ 10.0, 15.0, 16.0 at Dean number $(D_n) = 500, 1000, 1500$ and 2000 respectively.

In Figures (10)-(13), the secondary flow, solid lines solid lines $(\psi \geq 0)$ show that the secondary flow is the counter clock wise direction and the dotted ones $(\psi < 0)$ show that the secondary flow is in the clock wise direction. We have observed that the symmetric solution is obtained in the range $50 \leq T_r \leq 32000$.

The stream lines of the secondary flow have been shown at various Taylor number (T_r) in the development of the vortex. 2-vortex solution has been found at $T_r = 20000$ and 3-vortex solution has been found at $T_r = 16000$ as well as 4-vortex solution has been obtained at $T_r = 1000, 1300, 2000, 2300, 3000, 3500, 3700, 5500, 8000, 10000$ (see Figure 10); 2-vortex solution has been found at $T_r = 16000$ and 3-vortex solution have been found at $T_r = 3300, 5000, 7000, 8000$ as well as 4-vortex solution has been found at $T_r = 1000, 1500, 2500, 3000, 3500, 3700, 4700, 5000,$ (see Figure 11); 3-vortex solution has been found at $T_r = 2000$ and 4-vortex solution have been obtained at $T_r = 1000, 1500, 2500, 3000,$ $3500, 3700, 4700, 5000, 7000, 8000$ (see Figure 12); 3-vortex solutions have been found at $T_r = 8000, 16000$ and 4-vortex solutions have been found at $T_r = 1000, 1300, 2000, 2700, 3000, 3700, 4700, 5300, 5700$ (see Figure 13) in the secondary flow.

The contour plots of the axial flow has been formed the ring which are either single or double ring shape that appeared depends on the various Taylor number (T_r) as well as Magnetic parameter (M_g). Single nine rings are found at $T_r = 16000$ and 32000 where Dean number $(D_n) = 500$ in Figure 10; triple nine rings are found at $T_r = 8000$ and double rings has been found at $T_r = 16000, 24000, 32000$ at Dean number $(D_n) = 1000, 1500$ and 2000 respectively.

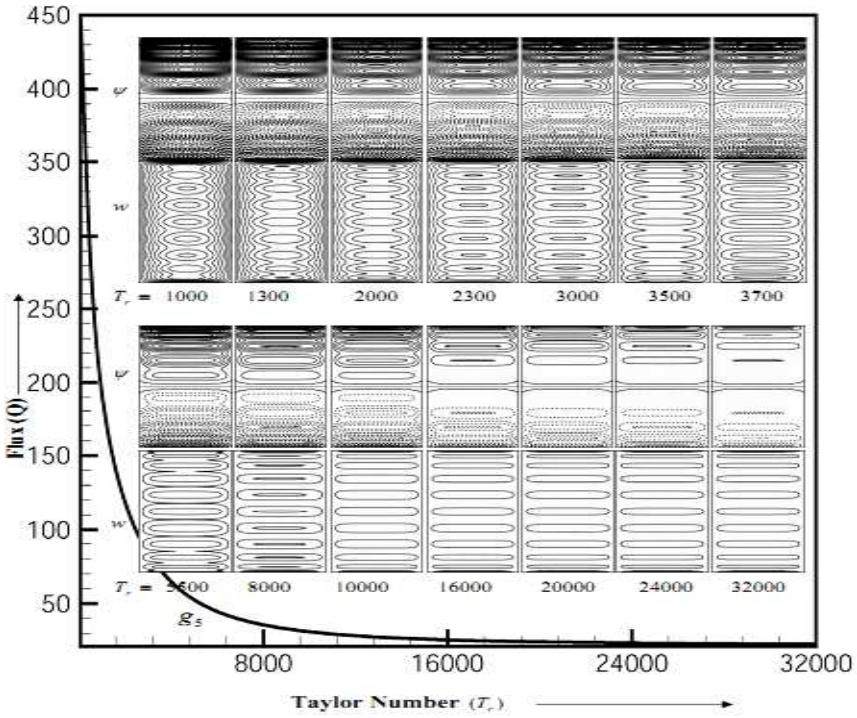

Figure 10: Stream Lines of the Secondary Flow (Top) and Contours Plot of Axial Flow (Bottom) in Each Row at Dean Number $(D_n) = 500$ and $M_g = 4000$ for Flux (Q) versus Taylor Number (T_r) at $T_r = 1000, 1300, 2000, 2300, 3000, 3500, 3700, 5500, 8000, 10000, 16000, 20000, 24000, 32000$

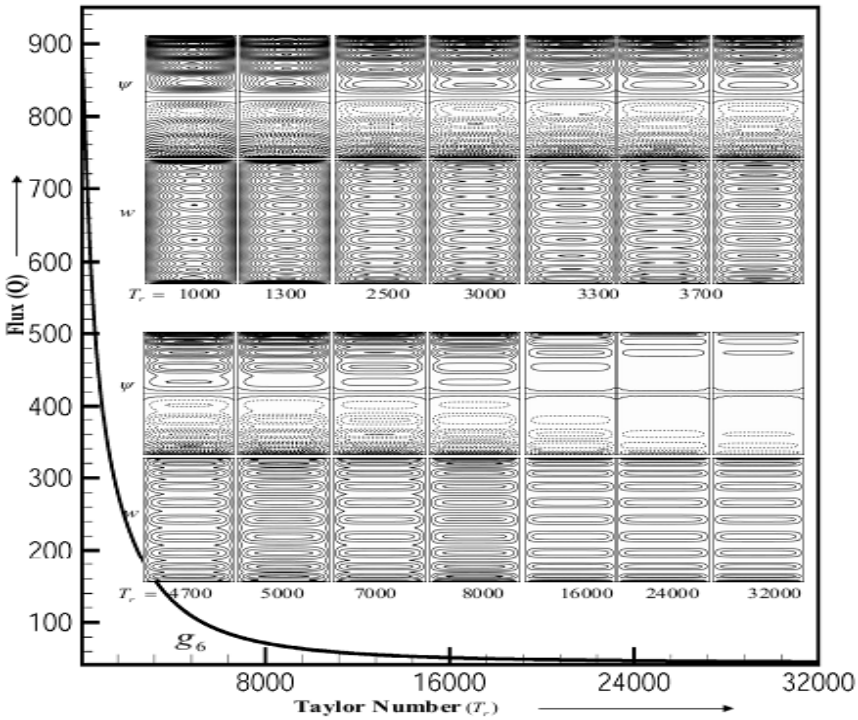

Figure 11: Stream Lines of the Secondary Flow (Top) and Contours Plot of Axial Flow (Bottom) in Each Row at Dean Number $(D_n) = 1000$ and $M_g = 4000$ for Flux (Q) versus Taylor Number (T_r) at $T_r = 1000, 1300, 2500, 3000, 3300, 3700, 4000, 4700, 5000, 7000, 8000, 16000, 24000, 32000$

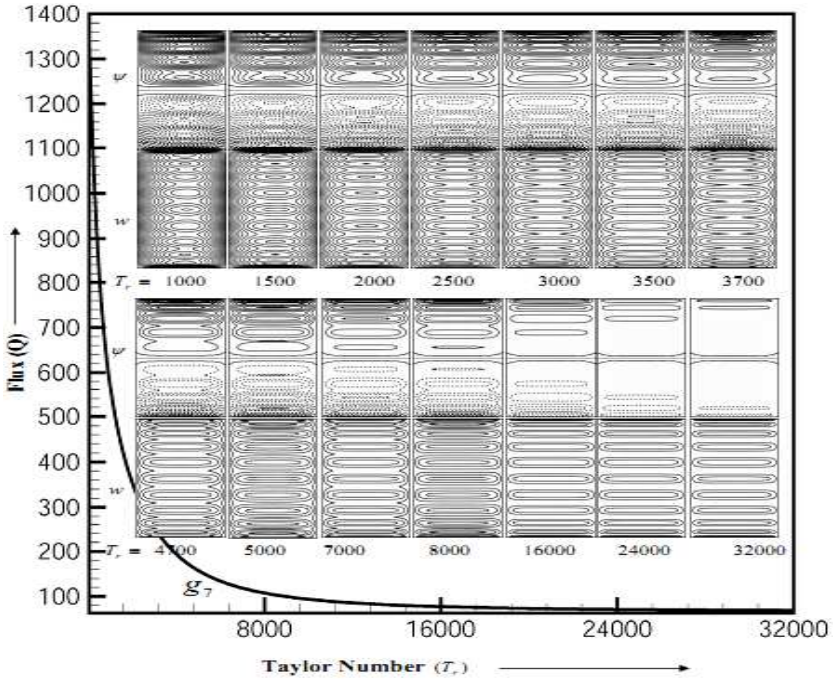

Figure 12: Stream Lines of the Secondary Flow (Top) and Contours Plot of Axial Flow (Bottom) in Each Row at Dean Number $(D_n) = 1500$ and $M_g = 4000$ for Flux (Q) versus Taylor Number (T_r) at $T_r = 1000, 1500, 2000, 2500, 3000, 3500, 3700, 4700, 5000, 7000, 8000, 16000, 24000, 32000$

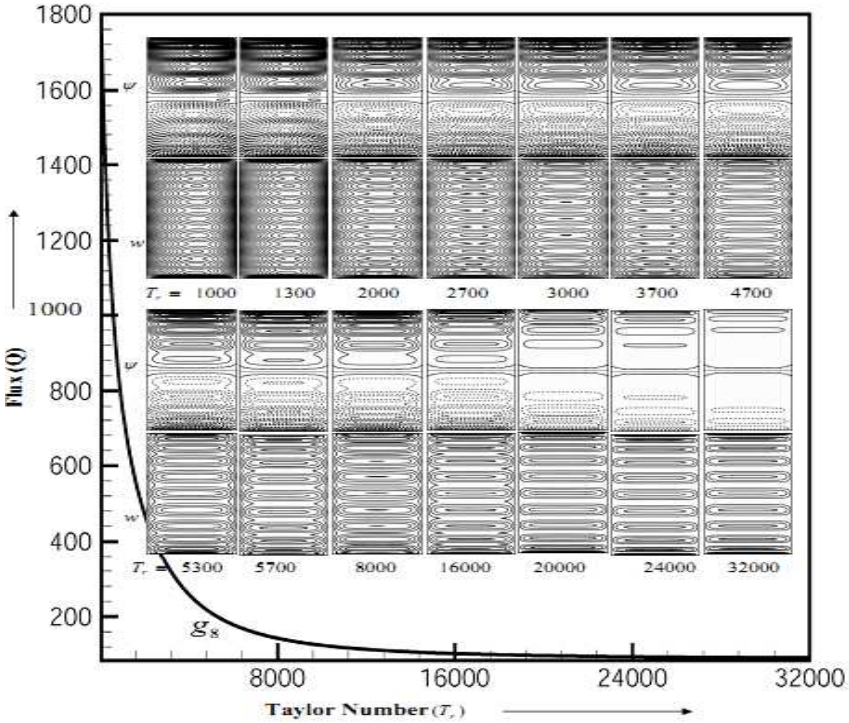

Figure 13: Stream Lines of the Secondary Flow (top) and Contours Plot of Axial Flow (Bottom) in Each Row at Dean Number $(D_n) = 2000$ and $M_g = 4000$ for Flux (Q) versus Taylor Number

Case III: $M_g = 3000$

The steady solution curves have been obtained for aspect ratio $(\gamma) = 2.0$ and $M_g = 3000$ in the range $50 \le T_r \le 32000$ which has been shown in the Figures (14)-(17). These solution curves have been denoted by g_9, g_{10}, g_{11} and g_{12} at the Dean number $(D_n) = 500$, 1000, 1500 and 2000 respectively for the graph of the total flux (Q) versus Taylor number (T_r). The flow patterns of the secondary flow and contours plot of the axial flow at several Taylor number (T_r) on the solution curve for constant ψ and w which has been shown by Figures (14)-(17). We look at the figures from the upstream. Therefore in these figures, we can understand the structures of the secondary flow and the axial flow. We take $T_r =$ (1000, 1500, 1700, 2000, 2500, 3000, 3500, 3700, 5500, 5700, 8000, 16000, 24000 and 32000) on g_9 curve (see Figure 14); $T_r =$ (1000, 2000, 2300, 2500, 2700, 3000, 3500, 3700, 4700, 7000, 8000, 16000, 24000 and 32000) on g_{10} curve (see Figure 15); $T_r =$ (1000, 2000, 2500, 2700, 3000, 3700, 4000, 4700, 5000, 7000, 8000, 16000, 24000 and 32000) on g_{11} curve (see Figure 16); $T_r =$ (1000, 1500, 2000, 2500, 2700, 3500, 3700, 4000, 5500, 7000, 8000, 16000, 24000 and 32000) on g_{12} curve (see Figure 17) where the stream lines of the secondary flow (top) and the contour plots of the axial flow (bottom) in each row from left to the right with the increment $\Delta\psi =$ 0.030, 0.050, 0.090, 0.10 and $\Delta w =$ 8.0, 10.0, 14.5, 16.0 at Dean number $(D_n) = 500$, 1000, 1500 and 2000 respectively. In Figures (14)-(17), the secondary flow, solid lines solid lines $(\psi \ge 0)$ show that the secondary flow is the counter clock wise direction and the dotted ones $(\psi < 0)$ show that the secondary flow is in the clock wise direction. We have observed that the symmetric solution has obtained in the range $50 \le T_r \le 32000$. The stream lines of the secondary flow have been shown at various Taylor number (T_r) in the development of the vortex. 3-vortex solutions have been found at $T_r = 1000$, 3000 and 4-vortex solutions have been obtained at $T_r =$ 1700, 2500, 3500, 3700, 5500, 5700, 8000, 9000 as well as 5-vortex solution has been found at $T_r = 2000$, 1500 (see Figure 14); 2-vortex solution has been found at $T_r = 1000$ and 3- vortex solution have been obtained at $T_r = 7000$, 8000 as well as 4-vortex solutions have been found at $T_r = 1000$, 2000, 2300, 2500, 2700, 3000, 3500, 3700 and 4700 (see Figure 15); 2-vortex solution has been found at $T_r = 16000$, 3-vortex solutions have been obtained at $T_r = 1000$, 2000, 2700, 3000, 4700, 5000, 7000, 8000 and 4-vortex solutions have been found at $T_r = 2500$, 3700, 4000 (see Figure 16); 2-vortex solution has been found at $T_r = 16000$, 3-vortex solutions have been obtained at $T_r = 2000$, 3500, 5500, 7000, 8000, 4-vortex solutions have been found at $T_r = 2500$, 2700, 3700, 4000 and 5-vortex solution has obtained at $T_r = 1500$. The contour plots of the axial flow has been formed the ring which are either single or double ring shape that appeared depends on the various Taylor number (T_r) as well as Magnetic parameter (M_g). Single nine rings are found at $T_r = 9000$,16000 and 32000 and double rings are found at $T_r =$ 5700 where Dean number $(D_n) = 500$ in Figure 14; triple rings are found at $T_r = 8000$ and double rings are found at $T_r =$ 16000,24000, 32000 at Dean number $(D_n) =$ 1000, 1500 and 2000 respectively.

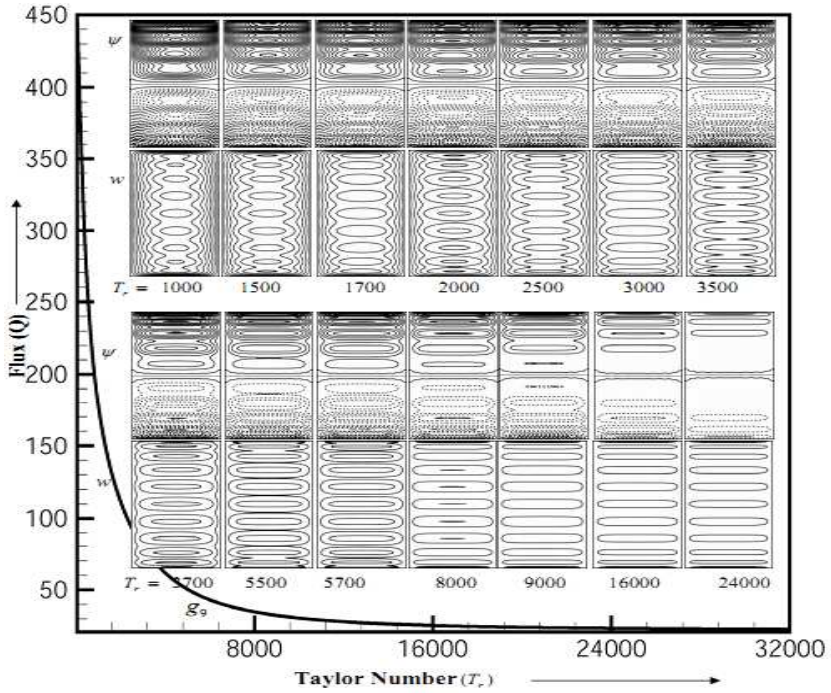

Figure 14: Stream Lines of the Secondary Flow (top) and Contours Plot of Axial Flow (Bottom) in Each Row at Dean Number $(D_n) = 500$ and $M_g = 3000$ for Flux (Q) versus Taylor Number (T_r) at $T_r = 1000, 1500, 1700, 2000, 2500, 3000, 3500, 3700, 5500, 5700, 8000, 9000, 16000, 24000$

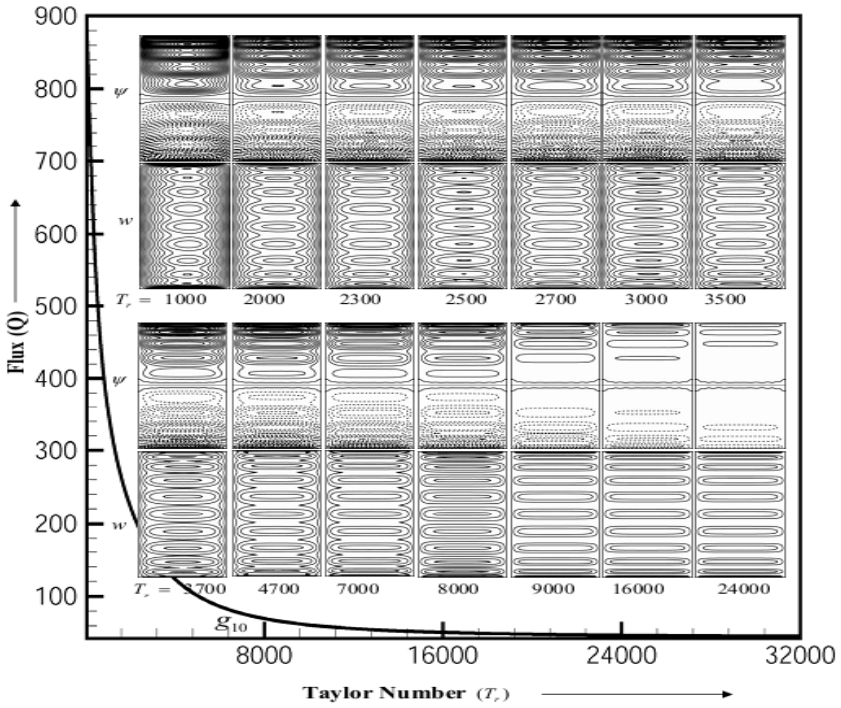

Figure 15: Stream Lines of the Secondary Flow (top) and Contours Plot of Axial Flow (Bottom) in Each Row at Dean Number $(D_n) = 1000$ and $M_g = 3000$ for Flux (Q) versus Taylor Number (T_r) at $T_r = 1000, 2000, 2300, 2500, 2700, 3000, 3500, 3700, 4700, 7000, 8000, 9000, 16000, 24000$

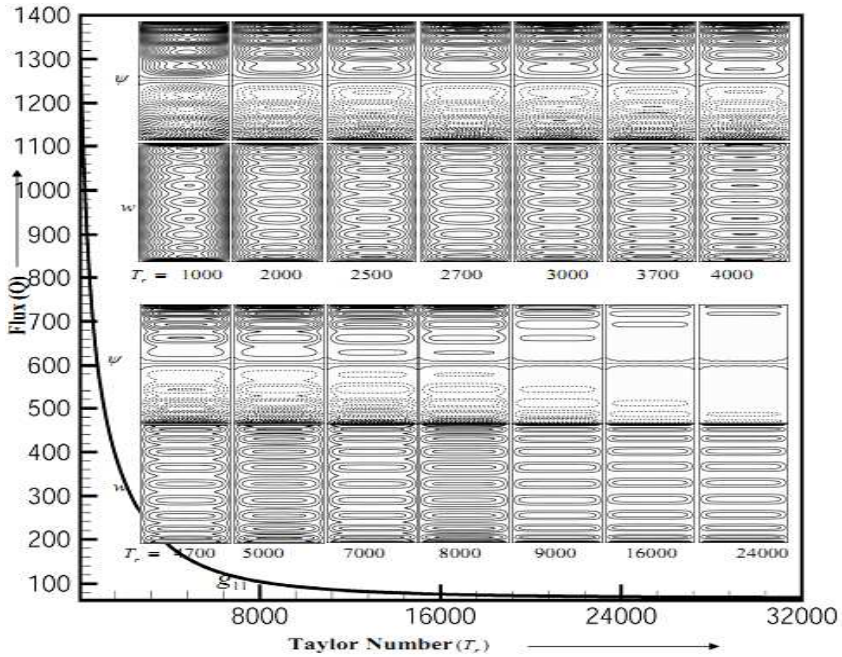

Figure 16: Stream Lines of the Secondary Flow (Top) and Contours Plot of Axial Flow (Bottom) in Each Row at Dean Number $(D_n) = 1500$ and $M_g = 3000$ for Flux (Q) versus Taylor Number (T_r) at $T_r = 1000, 2000, 2500, 2700, 3000, 3700, 4000, 4700, 5000, 7000, 8000, 9000, 16000, 24000$

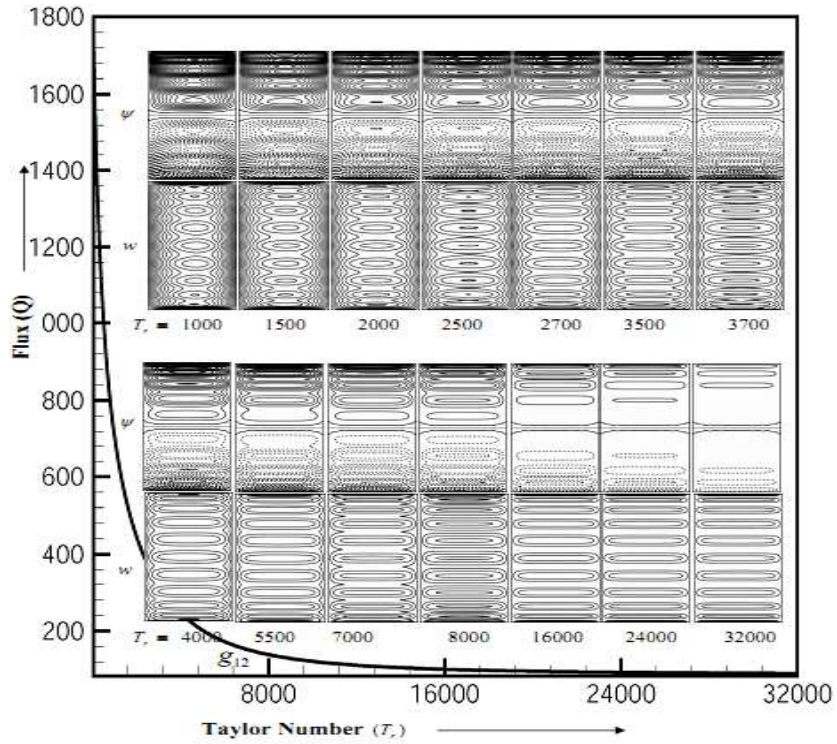

Figure 17: Stream Lines of the Secondary Flow (Top) and Contours Plot of Axial Flow (Bottom) in Each Row at Dean Number $(D_n) = 2000$ and $M_g = 3000$ for Flux (Q) versus Taylor Number (T_r) at $T_r = 1000, 1500, 2000, 2500, 2700, 3500, 3700, 4000, 5500, 7000, 8000, 16000, 24000, 32000$

CONCLUSIONS

Based on the current results the following conclusions are made:

- At high Dean number (D_n) , for both cases of large Magnetic parameter (M_g) and Taylor number (T_r) the steady solution have been obtained.
- 2-vortex, 3-vortex, 4-vortex, 5-vortex and 6-vortex solutions have been found in the maximum secondary flow pattern which depends on the Magnetic parameter (M_g) and Taylor number (T_r) .
- The contour plots of the axial flow structures which have been turned into the single, double and triple ring shape that appeared depends on the various Taylor number (T_r) as well as Magnetic parameter (M_g) at Dean number $(D_n) = 500$, 1000, 1500 and 2000.

REFERENCES

1. Alam, Begum and Yamamato (2007), "Flow through a rotating straight pipe with large aspect ratio", *Journal of Energy, Heat and Mass Transfer*, vol 29, 153-173
2. Barua, S. N. (1955), "Secondary flow in rotating straight pipe", *Proceeding of Royal Society of London A.,* 227, 133-139.
3. Benton, U.S. and Baltimore, M.D. (1956), "The effect of the earth's rotation on laminar flow in pipes", *Journal of Applied Mechanics*, March Issue, 123-127.
4. Bara, B. Nandakumar, K. and Masliyah, J.H. (1992), "An experimental and numerical study of Dean problem: flow development towards two-dimensional multiple solutions", *Journal of Fluid Mechanics*, 244, 339-376.
5. Duck, P. W. (1983), "Flow through rotating straight pipes of a circular cross- section", *Physics of Fluids A*, 26(3), 624-618.
6. Dousset, V. (2009), "Numerical solutions of MHD flows past obstacles in a duct under externally applied magnetic field", *Ph.D thesis, Coventry University.*
7. *Faraday, M.* (1832), "Experimental Researches in electrically" *Phill. Trans., **15**, 175.*
8. Gotlieb, D. and Orszag, S.A. (1977), "Numerical Analysis of Spectral Methods, *Society for Industrial and Applied Mathematics, Philadelphia.*
9. Ito, H. (1969), "Laminar flow in curved pipes", *Zeitschrift for Angewandte Mathematics and Mechanics, ZAMM,49,653-663.*
10. Ito, H. and Nanbu, K. (1971), "Flow in rotating straight pipes of circular cross-section", *ASME Journal of Basic Engineering*, September Issue, 383-394.
11. Lei, U. and Hsu, C. H. (1990), "Flow through a straight pipes", *Physics of Fluids A*, 2(1), 63-75.
12. Mansour, K. (1985), "Laminar flow through a slowly a rotating straight pipe", *Journal of Fluid Mechanics*, 150, 1-21.